

Sparse superposition codes with rotational invariant coding matrices for memoryless channels

YuHao Liu[†], Teng Fu[†], Jean Barbier[◇] and TianQi Hou^{*}

[†] Department of Mathematical Sciences, Tsinghua University, Beijing, China

[◇] International Center for Theoretical Physics, Trieste, Italy

^{*} Theory Lab, Central Research Institute, 2012 Labs, Huawei Technologies Co., Ltd.

Emails: {yh-liu21, fut21}@mails.tsinghua.edu.cn, jbarbier@ictp.it, thou@connect.ust.hk

Abstract—We recently showed in [1] the superiority of certain structured coding matrices ensembles (such as partial row-orthogonal) for sparse superposition codes when compared with purely random matrices with i.i.d. entries, both information-theoretically and under practical vector approximate message-passing decoding. Here we generalize this result to binary input channels under generalized vector approximate message-passing decoding [2]. We focus on specific binary output channels for concreteness but our analysis based on the replica symmetric method from statistical physics applies to any memoryless channel. We confirm that the “spectral criterion” introduced in [1], a coding-matrix design principle which allows the code to be capacity-achieving in the “large section size” asymptotic limit, extends to generic memoryless channels. Moreover, we also show that the vanishing error floor property [3] of this coding scheme is universal for arbitrary spectrum of the coding matrix.

I. INTRODUCTION

Since their introduction [4] and proof of capacity-achievability [5–7] for communication over the additive white gaussian noise (AWGN) channel, sparse superposition (SS) codes have become an active research field given their practical potential [8], in particular under approximate message-passing (AMP) decoding [7, 9]. But the application range of SS codes has been strongly expanded once it was realized that their desirable properties are universally true for generic memoryless channels when a proper generalization of AMP is employed as a decoder [3, 10]. Even more recently, following similar studies in the related area of compressive sensing [11–14], we have initiated the analysis of SS codes with more generic coding matrices than with i.i.d. entries as is usually the case [1], but for the AWGN channel only. In the present contribution we go much beyond by extending these latter results to generic memoryless channels. Our main result comes in the form of a simple criterion for the “optimal” design among a large class of rotationally-invariant coding matrices, yielding a code which is capacity achieving. Moreover we introduce and analyse the performance of a decoder for SS codes based on the generalized vector approximate message-passing algorithm (GVAMP) [2]. We also show that when decoding is successful it is (asymptotically, but also empirically) perfect for binary input channels: *there is no error-floor*, a very desirable property for any coding scheme. To be concrete we focus on three paradigmatic memoryless channels: the binary erasure (BEC) and symmetric (BSC) channels, and the (non-

symmetric) Z channel (ZC). But our theory applies to more generic memoryless channels.

Like in [1] our non-rigorous analysis is based on a careful study of the potential function derived from the replica method [15] and its connection to the fixed point(s) of the state evolution (SE) recursions tracking AMP-like algorithms [16–19]. Nevertheless, a multitude of rigorous studies [7, 10, 13, 20–22] point towards the fact that our predictions should be exact in a proper asymptotic limit. Moreover we empirically confirm through careful numerics that our replica-based theory accurately predicts GVAMP’s performance (i.e., its mean-square error (MSE) after convergence). Therefore our results must be considered as numerically-verified conjectures based on by-now well established techniques from statistical physics.

In SS codes, the *message* $\mathbf{x} = [\mathbf{x}_1, \dots, \mathbf{x}_L]$ is a vector made of L B -dimensional *sections*. Each section \mathbf{x}_l , $l \in \{1, \dots, L\}$ possesses a single non-zero component equal to 1 whose position encodes the symbol to transmit. B is the *section size* (or alphabet size) and we set $N := LB$. We consider random codes generated by a *coding matrix* $\mathbf{A} \in \mathbb{R}^{M \times N}$ drawn from a rotational invariant ensemble, i.e., when considering its singular value decomposition $\mathbf{A} = \mathbf{U}\sqrt{\mathbf{S}}\mathbf{V}^\top$, the orthogonal basis of singular vectors \mathbf{U} and \mathbf{V} are sampled uniformly in the orthogonal group $\mathcal{O}(M)$ and $\mathcal{O}(N)$, respectively. The diagonal matrix \mathbf{S} contains non-negative singular values $(S_i)_{i \leq N}$ on its main diagonal, and whose empirical distribution $N^{-1} \sum_{i \leq N} \delta_{S_i}$ weakly converges to a well-defined compactly supported probability density function $\nu(\lambda)$ as $N, M \rightarrow \infty$ (not necessarily proportionally). We denote its aspect ratio $\alpha = M/N$. The cardinality of the code is B^L . Hence, the (design) rate is $R = L \log_2(B)/M = \log_2(B)/(\alpha B)$ and thus the code is fully specified by (M, R, B) . For a message \mathbf{x} as before, the *codeword* is $\mathbf{Ax} \in \mathbb{R}^M$. We enforce the power constraint $\|\mathbf{Ax}\|_2^2/M = 1 + o_L(1)$ by tuning the spectrum $\nu(\lambda)$ to satisfy $\int d\lambda \lambda \nu(\lambda) = \alpha B$. The asymptotic spectral density of $B^{-1} \mathbf{A}^\top \mathbf{A}$ reads is written $\rho = (1 - \alpha)\delta_0 + \alpha\rho_{\text{supp}}$. The channel P_{out} outputs the noisy codeword $\mathbf{y} = (y_\mu)_{\mu \leq M}$. For the *memoryless* channels we focus on, $P_{\text{out}}(y_\mu | [\mathbf{Ax}]_\mu)$ is expressed as follows:

- BEC: $(1 - \epsilon)\delta(y_\mu - \text{sign}([\mathbf{Ax}]_\mu)) + \epsilon\delta(y_\mu)$,
- BSC: $(1 - \epsilon)\delta(y_\mu - \text{sign}([\mathbf{Ax}]_\mu)) + \epsilon\delta(y_\mu + \text{sign}([\mathbf{Ax}]_\mu))$,
- ZC: $\delta(\text{sign}([\mathbf{Ax}]_\mu) + 1)(\epsilon\delta(y_\mu - 1) + (1 - \epsilon)\delta(y_\mu + 1)) + \delta(\text{sign}([\mathbf{Ax}]_\mu) - 1)\delta(y_\mu - 1)$,

where ϵ represents the error probability. The only error performances measure we are going to analyse is the MSE per section $L^{-1}\mathbb{E}\|\mathbf{x} - \hat{\mathbf{x}}(\mathbf{y}, \mathbf{A})\|_2^2$ where $\hat{\mathbf{x}}(\mathbf{y}, \mathbf{A})$ will be either the minimum mean-square (MMSE) or GVAMP estimator.

II. GVAMP-BASED DECODER FOR SS CODES

The GVAMP we propose aims at computing the MMSE estimator $\mathbb{E}[\mathbf{x} | \mathbf{y}, \mathbf{A}]$ given by the mean of the posterior

$$P(\mathbf{x} | \mathbf{y}, \mathbf{A}) = \frac{1}{\mathcal{Z}(\mathbf{y}, \mathbf{A})} \prod_{\mu=1}^M P_{\text{out}}(y_\mu | [\mathbf{A}\mathbf{x}]_\mu) \prod_{l \leq L} P_0(\mathbf{x}_l),$$

where $\mathcal{Z}(\mathbf{y}, \mathbf{A})$ is a normalization. The hard constraints for the sections of the message are enforced by the prior distribution $P_0(\mathbf{x}_l) = B^{-1} \sum_{i \in l} \delta_{x_i, 1} \prod_{j \in l, j \neq i} \delta_{x_j, 0}$, where $\{i \in l\}$ are the B scalar components indices of the section l . GVAMP was originally derived for generalized linear estimation [2]. The present generalization to the vectorial setting of SS codes is in the same spirit as the one of AMP for SS codes found in [23]: only the input non-linear step differs from the canonical GVAMP, where the so-called denoiser $\mathbf{g}_1(\mathbf{r}, \gamma)$ (which takes into account the prior P_0) acts now *section-wise* instead of component-wise. Other than this, the decoder is the standard GVAMP. In full generality, it is $\mathbf{g}_1(\mathbf{r}, \gamma) := \mathbb{E}[\mathbf{X} | \mathbf{R} = \mathbf{r}]$ for the random variable $\mathbf{R} = \mathbf{X} + \sqrt{\gamma}\mathbf{Z}$ with $\mathbf{X} \sim P_0^{\otimes L}$ and $\mathbf{Z} \sim \mathcal{N}(0, \mathbf{I}_N)$. Plugging P_0 yields the component-wise expression of the denoiser and its variance:

$$\begin{cases} [\mathbf{g}_{x1}(\mathbf{r}, \gamma)]_i & := \frac{\exp((2r_i - 1)/(2\gamma))}{\sum_{j \in l_i} \exp((2r_j - 1)/(2\gamma))}, \\ [\mathbf{g}'_{x1}(\mathbf{r}, \gamma)]_i & := \gamma^{-1} [\mathbf{g}_{x1}(\mathbf{r}, \gamma)]_i (1 - [\mathbf{g}_{x1}(\mathbf{r}, \gamma)]_i), \end{cases}$$

where $[\mathbf{g}'_{x1}(\mathbf{r}, \gamma)]_i := [\nabla_{\mathbf{r}} \mathbf{g}_{x1}(\mathbf{r}, \gamma)]_i$, l_i is the section to which belongs the i^{th} scalar component. For the auxiliary variable $\mathbf{z} = \mathbf{A}\mathbf{x}$, in contrast with \mathbf{g}_{x1} that only depends on P_0 , \mathbf{g}_{1z} and \mathbf{g}'_{1z} depend on the communication channel model and act component-wise. Their expressions are

$$\mathbf{g}_{z1}(\mathbf{p}, \tau) := \mathbb{E}_{p\mathbf{z}} \quad \mathbf{g}'_{z1}(\mathbf{p}, \tau) := \mathbf{Cov}_{p\mathbf{z}},$$

where the expectation and covariance matrix are taken with respect to $p(\mathbf{z} | \mathbf{y}) \propto P_{\text{out}}(\mathbf{y} | \mathbf{z})\mathcal{N}(\mathbf{z}; \mathbf{p}, \mathbf{I}/\tau)$ (where $\mathcal{N}(z; a, b)$ is the probability density function of the normal distribution with mean a and covariance b). The LMMSE estimators \mathbf{g}_{x2} and \mathbf{g}_{z2} are related to the following pseudo linear model: $\bar{\mathbf{y}} = \bar{\mathbf{A}}\bar{\mathbf{x}} + \bar{\mathbf{w}}$ where $\bar{\mathbf{y}} := \mathbf{0}$, $\bar{\mathbf{A}} := [\mathbf{A} - \mathbf{I}_M]$, $\bar{\mathbf{x}} := \begin{bmatrix} \mathbf{x} \\ \mathbf{z} \end{bmatrix}$, and $\bar{\mathbf{w}} \sim \mathcal{N}(\mathbf{0}, \mathbf{I}_M/\gamma_e)$ with prior $\bar{\mathbf{x}} \sim \mathcal{N}(\begin{bmatrix} \mathbf{r}_{2k} \\ \mathbf{p}_{2k} \end{bmatrix}, \begin{bmatrix} \mathbf{I}_N/\gamma_{2k} & \mathbf{0} \\ \mathbf{0} & \mathbf{I}_M/\tau_{2k} \end{bmatrix})$. The LMMSE estimate is $\int d\bar{\mathbf{x}} \bar{\mathbf{x}} p(\bar{\mathbf{x}} | \bar{\mathbf{y}})$, where $p(\bar{\mathbf{x}} | \bar{\mathbf{y}}) \propto p(\bar{\mathbf{y}} | \bar{\mathbf{x}})p(\bar{\mathbf{x}})$. Then in the limit $\gamma_e \rightarrow \infty$ strictly enforcing $\mathbf{z} = \mathbf{A}\mathbf{x}$, the LMMSE estimate and its variances read [2]

$$\begin{cases} \mathbf{g}_{x2}(\mathbf{r}_{2,k}, \mathbf{p}_{2,k}, \gamma_{2,k}, \tau_{2,k}) & := \mathbf{K}^{-1}(\tau_{2,k} \mathbf{A}^\top \mathbf{p}_{2,k} + \gamma_{2,k} \mathbf{r}_{2,k}), \\ \mathbf{g}_{z2}(\mathbf{r}_{2,k}, \mathbf{p}_{2,k}, \gamma_{2,k}, \tau_{2,k}) & := \mathbf{A} \mathbf{g}_{x2}(\mathbf{r}_{2,k}, \mathbf{p}_{2,k}, \gamma_{2,k}, \tau_{2,k}), \end{cases}$$

where $\mathbf{K} := \tau_{2,k} \mathbf{A}^\top \mathbf{A} + \gamma_{2,k} \mathbf{I}$. Moreover we have

$$\begin{cases} \mathbf{g}'_{x2}(\mathbf{r}_{2,k}, \mathbf{p}_{2,k}, \gamma_{2,k}, \tau_{2,k}) & = \gamma_{2,k} \mathbf{K}^{-1} \\ \mathbf{g}'_{z2}(\mathbf{r}_{2,k}, \mathbf{p}_{2,k}, \gamma_{2,k}, \tau_{2,k}) & = \tau_{2,k} \mathbf{A} \mathbf{K}^{-1} \mathbf{A}^\top. \end{cases}$$

where the prime $'$ means derivative w.r.t. the first argument, and $\langle M \rangle = k^{-1} \text{Tr } M$, $M \in \mathbb{R}^{k \times k}$.

Algorithm 1 GVAMP-based decoder for SS codes

Require: Max iteration K , coding matrix \mathbf{A} , observed \mathbf{y}

- 1: Initialize $\mathbf{r}_{1,0}, \mathbf{p}_{1,0}, \gamma_{1,0} > 0, \tau_{1,0} > 0$.
 - 2: **for** $k = 0, 1, \dots, K$ (or until convergence) **do**
 - 3: // Denoising \mathbf{x}
 - 4: $\hat{\mathbf{x}}_{1,k} = \mathbf{g}_{x1}(\mathbf{r}_{1,k}, \gamma_{1,k}), \quad \alpha_{1,k} = \langle \mathbf{g}'_{x1}(\mathbf{r}_{1,k}, \gamma_{1,k}) \rangle$
 - 5: $\mathbf{r}_{2,k} = (\hat{\mathbf{x}}_{1,k} - \alpha_{1,k} \mathbf{r}_{1,k}) / (1 - \alpha_{1,k})$
 - 6: $\gamma_{2,k} = \gamma_{1,k} (1 - \alpha_{1,k}) / \alpha_{1,k}$
 - 7: // Denoising \mathbf{z}
 - 8: $\hat{\mathbf{z}}_{1,k} = \mathbf{g}_{z1}(\mathbf{p}_{1,k}, \tau_{1,k}), \quad \beta_{1,k} = \langle \mathbf{g}'_{z1}(\mathbf{p}_{1,k}, \tau_{1,k}) \rangle$
 - 9: $\mathbf{p}_{2,k} = (\hat{\mathbf{z}}_{1,k} - \beta_{1,k} \mathbf{p}_{1,k}) / (1 - \beta_{1,k})$
 - 10: $\tau_{2,k} = \tau_{1,k} (1 - \beta_{1,k}) / \beta_{1,k}$
 - 11: // LMMSE estimation of \mathbf{x}
 - 12: $\hat{\mathbf{x}}_{2,k} = \mathbf{g}_{x2}(\mathbf{r}_{2,k}, \mathbf{p}_{2,k}, \gamma_{2,k}, \tau_{2,k})$
 - 13: $\alpha_{2,k} = \langle \mathbf{g}'_{x2}(\mathbf{r}_{2,k}, \mathbf{p}_{2,k}, \gamma_{2,k}, \tau_{2,k}) \rangle$
 - 14: $\mathbf{r}_{1,k+1} = (\hat{\mathbf{x}}_{2,k} - \alpha_{2,k} \mathbf{r}_{2,k}) / (1 - \alpha_{2,k})$
 - 15: $\gamma_{1,k+1} = \gamma_{2,k} (1 - \alpha_{2,k}) / \alpha_{2,k}$
 - 16: // LMMSE estimation of \mathbf{z}
 - 17: $\hat{\mathbf{z}}_{2,k} = \mathbf{g}_{z2}(\mathbf{r}_{2,k}, \mathbf{p}_{2,k}, \gamma_{2,k}, \tau_{2,k})$
 - 18: $\beta_{2,k} = \langle \mathbf{g}'_{z2}(\mathbf{r}_{2,k}, \mathbf{p}_{2,k}, \gamma_{2,k}, \tau_{2,k}) \rangle$
 - 19: $\mathbf{p}_{1,k+1} = (\hat{\mathbf{z}}_{2,k} - \beta_{2,k} \mathbf{p}_{2,k}) / (1 - \beta_{2,k})$
 - 20: $\tau_{1,k+1} = \tau_{2,k} (1 - \beta_{2,k}) / \beta_{2,k}$
 - 21: **end for**
 - 22: Return $\hat{\mathbf{x}} = \hat{\mathbf{x}}_{1,K}$.
-

III. ASYMPTOTIC ANALYSIS BY THE REPLICA METHOD

The performance of SS codes in the $L \rightarrow \infty$ limit will be analyzed using the non-rigorous (yet conjectured exact) replica method – which, again, has been proved to be correct in many inference problems [13, 20–22, 24–26] – in order to obtain both the minimum mean-square error (MMSE) and GVAMP's fixed point performance. Note that we do *not* aim at tracking its per-iterate performance, which would instead require to use the rather involved state evolution analyses of [18, 19]. Actually, making SE rigorous for SS codes (a goal beyond the scope of the present paper) requires special care, see [7]. So even if we were to use the previous references to track GVAMP by state evolution, it would not really be rigorous (even if probably correctly tracking the decoder for any practical purpose) and so we would not gain much compared to our replica approach. Our choice of using the replica method only is thus that *i*) it allows to access both performance measures (algorithmic and information-theoretic), and *ii*) despite their apparent technicality, our replica equations remain simpler than GVAMP's state evolution [18, 19], the reason being that our equations focus on the fixed point rather than on dynamics.

A. Replica potential function

The goal of the replica method is to compute the so-called *free entropy* (i.e., log-partition function) $\Phi := \mathbb{E}_{\mathbf{y}, \mathbf{A}} \ln \mathcal{Z}(\mathbf{y}, \mathbf{A})$ using the ‘‘replica trick’’ $\mathbb{E} \ln \mathcal{Z} = \lim_{n \rightarrow 0} \partial_n \ln \mathbb{E} \mathcal{Z}^n$. For any fixed $B \geq 2$ we adapt the results of [19, 27, 28] for the standard GLM with generic rotational invariant matrices to SS codes, namely, we make the necessary changes required to go from a scalar setting ($B = 1$) to

the section-wise setting of SS codes ($B \geq 2$); the complete derivation will be reported in a longer version. The resulting variational formula reads

$$\Phi = \sup_{q_x \in [0, \frac{1}{B}], q_z \geq 0, \hat{q}_x \geq 0, \hat{q}_z \in [0, 1]} \inf_{\mathbf{S}, \mathbf{s}} \Phi_{\text{RS}}(q_x, q_z, \hat{q}_x, \hat{q}_z), \quad (1)$$

$$\Phi_{\text{RS}}(q_x, q_z, \hat{q}_x, \hat{q}_z) := I_0(q_x, \hat{q}_x) + \alpha I_{\text{out}}(q_z, \hat{q}_z) + I_{\text{int}}(q_x, q_z),$$

where the functions constructing the *replica potential* Φ_{RS} are

$$\begin{cases} I_0(q_x, \hat{q}_x) := \mathbb{E}_{\xi, \mathbf{s}} \ln \mathcal{Z}_0(\hat{q}_x, \mathbf{S}, \xi) - \frac{B}{2} q_x \hat{q}_x, \\ I_{\text{int}}(q_x, q_z) := B \mathcal{F}(1 - B q_x, q_z) + \frac{1}{2} \alpha B q_z, \\ I_{\text{out}}(q_z, \hat{q}_z) := B \mathbb{E}_{\xi} \int dy \mathcal{Z}_{\text{out}}(y; \hat{q}_z \xi, 1 - \hat{q}_z) \\ \quad \times \ln \mathcal{Z}_{\text{out}}(y; \hat{q}_z \xi, 1 - \hat{q}_z) - \frac{B}{2} q_z \hat{q}_z. \end{cases}$$

with $\xi \sim \mathcal{N}(0, 1)$, $\xi \sim \mathcal{N}(0, \mathbf{I}_B)$ and $\mathbb{R}^B \ni \mathbf{S}, \mathbf{s} \sim P_0$ all independently. The auxiliary functions are

$$\begin{cases} \mathcal{Z}_0(\hat{q}_x, \mathbf{S}, \xi) := \mathbb{E}_{\mathbf{s}} \exp\left(-\frac{\hat{q}_x}{2} \|\mathbf{s}\|_2^2 + \sqrt{\hat{q}_x} \mathbf{s}^\top (\sqrt{\hat{q}_x} \mathbf{S} + \xi)\right), \\ \mathcal{Z}_{\text{out}}(y; \omega, v) := \int dz P_{\text{out}}(y | z) \mathcal{N}(z; \omega, v), \end{cases}$$

and $\mathcal{F}(x, y)$ is the *rectangular spherical integral* used, e.g., in [29, 30] where it is expressed as follows:

$$2\mathcal{F}(x, y) := \inf_{\Lambda_x, \Lambda_y \geq 0} \left\{ (1 - \alpha) \ln \Lambda_y - \mathbb{E} \ln(\Lambda_x \Lambda_y + \lambda) + \Lambda_x x + \alpha \Lambda_y y - \ln x - \alpha \ln y - \alpha - 1 \right\}, \quad (2)$$

where $\lambda \sim \rho$ with ρ the asymptotic spectral density of $B^{-1} \mathbf{A}^\top \mathbf{A}$. For i.i.d gaussian ensembles, whose spectrum density is the Marcenko-Pastur (MP) law, $\mathcal{F}_{\text{MP}}(x, y) = -\frac{\alpha}{2} xy$; for the row-orthogonal ensemble with spectral density $\rho_{\text{row}} = (1 - \alpha)\delta_0 + \alpha\delta_1$ it is $\mathcal{F}_{\text{row}}(x, y) = -\frac{1}{2} \ln\left(\frac{1}{2}(1 + \sqrt{1 - 4\alpha xy})\right) + \frac{1}{2} \sqrt{1 - 4\alpha xy} - \frac{1}{2}$. So we have a decomposition of the potential into a part I_0 encoding information about the prior P_0 , I_{out} on the channel P_{out} and I_{int} on the coding ensemble (through ρ).

B. Stationary equations of the replica potential

Assuming that the various extrema of the above variational problems are attained inside the optimization domains, the coupled stationary equations obtained by setting $\nabla \Phi_{\text{RS}} = \mathbf{0}$ read (again $\mathbb{R}^B \ni \mathbf{s} \sim P_0$, $\xi \sim \mathcal{N}(0, \mathbf{I}_B)$ and $\xi \sim \mathcal{N}(0, 1)$)

$$\begin{cases} q_x = B^{-1} \mathbb{E}_{\mathbf{s}, \xi} \|\mathbb{E}[\mathbf{s} | \mathbf{y} = \sqrt{q_x} \mathbf{s} + \xi]\|_2^2 \\ q_z = \mathbb{E}_{\xi} \int dy \mathcal{Z}_{\text{out}}(y; \sqrt{\hat{q}_z} \xi, 1 - \hat{q}_z) \\ \quad \times |\partial_{\omega} \ln \mathcal{Z}_{\text{out}}(y; \omega, 1 - \hat{q}_z)|_{\omega = \sqrt{\hat{q}_z} \xi}|^2, \\ \hat{q}_x = 2 \partial_{q_x} \mathcal{F}(1 - B q_x, q_z), \\ \hat{q}_z = 1 + 2\alpha^{-1} \partial_{q_z} \mathcal{F}(1 - B q_x, q_z), \end{cases}$$

The above stationary conditions of the replica potential will be our main tool of analysis (we call the first the q_x -stationary equation, etc.). Indeed, a powerful feature of the variational formula (1) is that the associated stationary conditions can characterize both the MMSE and the MSE attained by the GVAMP algorithm after convergence, in the limit $L \rightarrow +\infty$ [18, 19] as we describe in the next section.

In particular, the ‘‘overlap’’ q_x physically corresponds to the inner product $\lim_{L \rightarrow +\infty} N^{-1} \mathbb{E}[\mathbf{x}^\top \hat{\mathbf{x}}]$ between the signal \mathbf{x} and $\hat{\mathbf{x}}$ that can be either the MMSE or GVAMP estimator.

Therefore, given one solution $(q_x, q_z, \hat{q}_x, \hat{q}_z)$ of the stationary equations (which, as we will see, can characterize both the MMSE or GVAMP estimators), the replica prediction for the corresponding asymptotic MSE per section is $1 - B q_x$. Simplifying the first stationary equation for q_x we get an equivalent expression of this MSE, which this time depends on \hat{q}_x , and that is more practical/stable when q_x becomes small:

$$E(\hat{q}_x) := \mathbb{E}_{\xi} [(f_1(\hat{q}_x, \xi) - 1)^2 + (B - 1) f_2(\hat{q}_x, \xi)^2], \quad (3)$$

$$\begin{cases} f_1(x, \xi) := (1 + e^{-x} \sum_{i=2}^B e^{\sqrt{x}(\xi_i - \xi_1)})^{-1}, \\ f_2(x, \xi) := (1 + e^{x + \sqrt{x}(\xi_1 - \xi_2)} + e^{\sum_{i=3}^B \sqrt{x}(\xi_i - \xi_2)})^{-1}. \end{cases} \quad (4)$$

For a solution $(q_x, q_z, \hat{q}_x, \hat{q}_z)$, $E(\hat{q}_x) = 1 - B q_x$, see [9].

C. Analyzing the replica stationary equations

The MMSE and GVAMP performances are obtained by iteratively solving the stationary equations starting from two distinct initial conditions: the *informative initialization* is ($q_{\text{in},x}^{t=0} = B^{-1}, q_{\text{in},z}^{t=0} > 0$) and gives access to solution $\mathbf{q}_{\text{in}} = (q_{\text{in},x}^{\infty}, q_{\text{in},z}^{\infty}, \hat{q}_{\text{in},x}^{\infty}, \hat{q}_{\text{in},z}^{\infty})$. Because of the aforementioned MSE- q_x connection, algorithmically this means ‘‘initializing on the solution’’, i.e., an oracle initialization with MSE $1 - B q_{\text{in},x}^{t=0} = 0$. Instead the *un-informative initialization* ($q_{\text{un},x}^{t=0} = 0, q_{\text{un},z}^{t=0} > 0$) yields the solution \mathbf{q}_{un} which verifies $q_{\text{un},x}^{\infty} \leq q_{\text{in},x}^{\infty}$. It corresponds to a practical initialization without knowledge of the signal. We empirically verified that only these two fixed points exist, independently of how $q_z > 0$ is initialized. This holds in more standard settings of SS codes [9]. With these two solutions in hand, one needs to plug each of them in the replica potential Φ_{RS} and compare the obtained values; the reason for that step is explained below. Denote $\Phi_{\text{in}} := \Phi_{\text{RS}}(\mathbf{q}_{\text{in}})$ and $\Phi_{\text{un}} := \Phi_{\text{RS}}(\mathbf{q}_{\text{un}})$ (keep in mind that these are functions of the rate R through their dependence on the fixed point(s), themselves dependent on R). In the replica theory, the MMSE is extracted from the fixed point with the highest free entropy (the so-called ‘‘thermodynamic equilibrium state’’ in physics parlance). So, denoting $\mathbf{q}_{\text{opt}} := \arg \max_{\mathbf{q} \in \{\mathbf{q}_{\text{in}}, \mathbf{q}_{\text{un}}\}} \Phi_{\text{RS}}(\mathbf{q})$, the replica prediction for the asymptotic MMSE is

$$\lim_{L \rightarrow +\infty} L^{-1} \mathbb{E} \|\mathbf{x} - \mathbb{E}[\mathbf{x} | \mathbf{y}, \mathbf{A}]\|_2^2 = 1 - B q_{\text{opt},x}^{\infty} = E(\hat{q}_{\text{opt},x}^{\infty}).$$

Instead, GVAMP’s MSE is given by plugging in it $\hat{q}_{\text{un},x}^{\infty}$:

$$\lim_{L \rightarrow +\infty} L^{-1} \mathbb{E} \|\mathbf{x} - \hat{\mathbf{x}}_{\text{GVAMP}}(\mathbf{y}, \mathbf{A})\|_2^2 = 1 - B q_{\text{un},x}^{\infty} = E(\hat{q}_{\text{un},x}^{\infty}).$$

This means that, as pointed in [18, 19], the fixed point of the state evolution recursions describing GVAMP’s MSE (and therefore its MSE for finite but large sizes L) can be accessed via the (simpler to implement) above equations. This is confirmed numerically, see Fig. 1.

Phase diagram for SS codes Depending on the rate R distinct regions exist and the transitions between them define two thresholds that can be extracted from the replica potential: the *GVAMP algorithmic threshold* R_{GVAMP} and the *information-theoretic threshold* R_{IT} :

$$R_{\text{GVAMP}} := \inf\{R: \Phi_{\text{un}} < \Phi_{\text{in}}\}, \quad R_{\text{IT}} := \sup\{R: \Phi_{\text{un}} < \Phi_{\text{in}}\}.$$

BEC	R_{GVAMP}^g	R_{IT}^g	R_{GVAMP}^r	R_{IT}^r
B=2	0.428	0.511	0.481	0.553
B=4	0.546	0.662	0.603	0.713
B=8	0.607	0.748	0.657	0.783
BSC	R_{GVAMP}^g	R_{IT}^g	R_{GVAMP}^r	R_{IT}^r
B=2	0.426	0.513	0.468	0.552
B=4	0.545	0.663	0.602	0.715
B=8	0.612	0.743	0.662	0.794
ZC	R_{GVAMP}^g	R_{IT}^g	R_{GVAMP}^r	R_{IT}^r
B=2	0.396	0.475	0.432	0.515
B=4	0.507	0.618	0.556	0.664
B=8	0.565	0.693	0.615	0.742

Table I. GVAMP threshold R_{GVAMP} and information theoretic threshold R_{IT} . The error probability ϵ for BEC, BSC and ZC is 0.1, 0.01 and 0.05 respectively. Superscript g and r signify gaussian matrix and row-orthogonal matrix respectively. Subscripts IT and GVAMP index the information-theoretic and algorithm thresholds, respectively.

Their analysis is one of our main goal. Equipped with the replica potential and these definitions, we describe the phase diagram (as R increases) using $\mathbf{q}_{\text{in}}, \mathbf{q}_{\text{un}}, \Phi_{\text{in}}, \Phi_{\text{un}}$:

- **Easy phase** $R < R_{\text{GVAMP}}$: In this region $\mathbf{q}_{\text{in}} = \mathbf{q}_{\text{un}}$ and thus GVAMP achieves the MMSE $1 - Bq_{\text{un},x}^\infty = E(\hat{q}_{\text{un},x}^\infty)$ which is “small”. Decoding is computationally efficient using GVAMP. At higher rate than R_{GVAMP} the fixed points differ and we enter the computationally hard phase. Threshold R_{GVAMP} corresponds to the rate where the the solid curve(s) jumps discontinuously on Fig. 1.

- **Hard phase** $R_{\text{GVAMP}} < R < R_{\text{IT}}$: In this region $\mathbf{q}_{\text{in}} \neq \mathbf{q}_{\text{un}}$ and $\Phi_{\text{un}} < \Phi_{\text{in}}$. GVAMP is sub-optimal, i.e., a statistical-to-computational gap is present. The MMSE equals $1 - Bq_{\text{in},x}^\infty = E(\hat{q}_{\text{in},x}^\infty)$ and is strictly lower than GVAMP’s MSE $1 - Bq_{\text{un},x}^\infty = E(\hat{q}_{\text{un},x}^\infty)$. Beyond R_{IT} the quality of inference becomes poor using any procedure, efficient or not.

- **Impossible phase** $R > R_{\text{IT}}$: \mathbf{q}_{in} may be equal or not to \mathbf{q}_{un} but the free entropy $\Phi_{\text{un}} > \Phi_{\text{in}}$ and $q_{\text{un},x}^\infty$ is “small”. In this case GVAMP is optimal and its MSE $1 - Bq_{\text{un},x}^\infty = E(\hat{q}_{\text{un},x}^\infty)$ (which matches the MMSE) is “large”.

The above scenario is generic in SS codes [3, 9] (and in high-dimensional inference more generically [22]), but it is also possible that no hard region is present at all (i.e., $R_{\text{IT}} = R_{\text{GVAMP}}$ and a single fixed point of the stationary equations exists for all rates). E.g., this happens at low SNR and/or low section size B for the AWGN channel. See [9] for the same phenomenology and plots for visualization.

IV. VANISHING ERROR FLOOR PROPERTY FOR $B < \infty$

The MSE floor E_f [3, 10] is the MSE attained from the informative initialization: $E_f := 1 - Bq_{\text{in},x}^\infty = E(\hat{q}_{\text{in},x}^\infty)$. In [3] it is shown that as $L \rightarrow \infty$ the error floor vanishes ($E_f = 0$) for any ϵ and B for a wide class of binary inputs channels, but only for i.i.d. gaussian coding matrix. We now heuristically show that *the vanishing error-floor property universally holds for rotationally invariant coding matrix ensembles with compactly supported spectra*. We focus on the BEC channel but the approach can be generalized to other binary input channels.

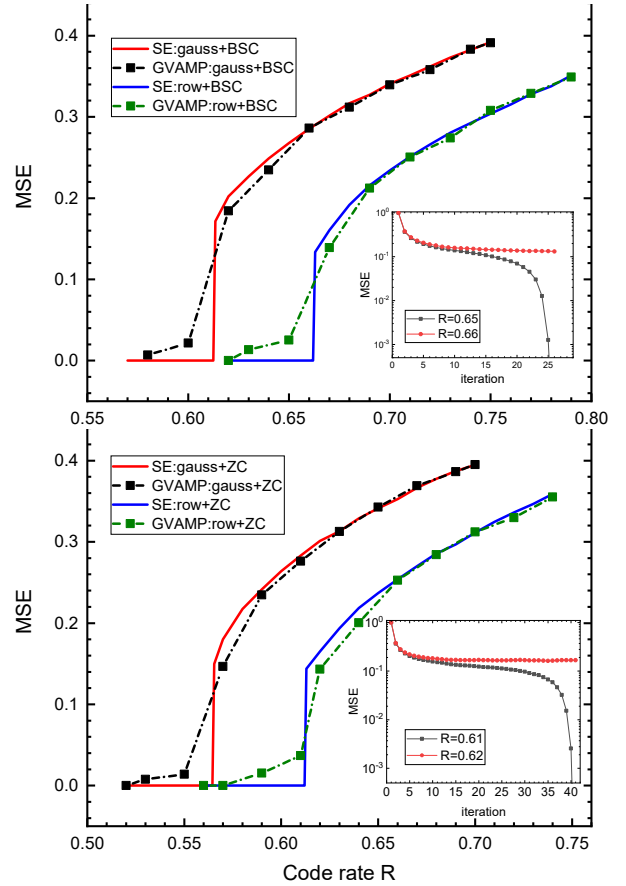


Fig. 1. The solid lines shows the GVAMP asymptotic fixed point MSE predicted from the replica stationary equations. The dashed dot lines are finite size performances of GVAMP over the BSC ($\epsilon = 0.01$) and ZC ($\epsilon = 0.05$) averaged over 50 instances with $L = 2^{14}$ and $B = 8$, as a function of the code rate R . The stationary equations are solved by Monte Carlo integration with 5×10^6 samples. Two types of coding matrices are considered: standard coding matrices with i.i.d. gaussian entries, and partial row-orthogonal ones. It is observed that as predicted by the theory the MSE error floor vanishes when the rate is smaller than their respective algorithmic threshold R_{GVAMP} , showed in table I. Clearly GVAMP performs better for row-orthogonal ensembles. The subfigures show the GVAMP iterates on one instance of size $L = 2^{14}$ and $B = 8$, with row-orthogonal matrices, as a function of the iterations.

Our strategy is to *assume* both *i*) the existence of a solution to the stationary equations such that $E_f = 0$, namely, such that $q_{\text{in},x}^\infty = B^{-1}$, and look for a self-consistent set of parameters values for the remaining stationary equations, and *ii*) this potential solution is such that the corresponding free entropy (Φ_{RS} evaluated in it) is the largest when a second solution exists, and this for all $R < R_{\text{IT}}$. The second hypothesis as well as the fact that only two solutions may co-exist have been thoroughly numerically verified in the present setting and previous ones [3]. From now on we drop unnecessary notations and simply denote \mathbf{q}_{in} by $(q_x, q_z, \hat{q}_x, \hat{q}_z)$. So we reverse engineer the solution starting from $q_x = B^{-1}$. Recall (3). from $E(\hat{q}_x) = 1 - Bq_x = 0$, $q_x = B^{-1}$ requires $\hat{q}_x = +\infty$ (this can be seen from the q_x -stationary equation too). When setting $(q_x = B^{-1}, \hat{q}_x = +\infty)$ in the \hat{q}_x -stationary equation we further deduce that $q_z = +\infty$. Indeed this is easily seen in the MP case: using $\mathcal{F}_{\text{MP}}(x, y) = -\frac{\alpha}{2}xy$

then $2\partial_{q_x}\mathcal{F}(1 - Bq_x, q_z) = B\alpha q_z$. Thus the \hat{q}_x -stationary equation becomes $+\infty = B\alpha q_z$ which implies $q_z = +\infty$. For general spectral law we use that, as shown in [29], $\mathcal{F}(x, y) = \mathcal{F}_{\text{MP}}(x, y) + O(x^2)$. And because $1 - Bq_x \rightarrow 0$ around the desired solution $q_x = B^{-1}$ the same argument applies: for any spectrum $(q_x = B^{-1}, \hat{q}_x = +\infty) \Rightarrow q_z = +\infty$. We finally need to fix the \hat{q}_z using the \hat{q}_z -stationary equation. Using the same approach, $\hat{q}_z = 1 + 2\alpha^{-1}\partial_{q_z}\mathcal{F}_{\text{MP}}(1 - Bq_x, q_z) = 1 - (1 - Bq_x) = Bq_x$ at the desired solution. So $(q_x = B^{-1}, \hat{q}_x = +\infty, q_z = +\infty, \hat{q}_z = 1)$ is a self-consistent solution *if and only if* it also verifies the last equation we did not exploit, namely the q_z -stationary equation.

Let $\mathcal{D}z$ be the standard gaussian measure. for the BEC channel the right-hand side of the q_z -stationary equation is

$$(1 - \epsilon)(2\pi\sqrt{1 - \hat{q}_z})^{-1} \int \mathcal{D}z \exp(-\frac{1}{2}\hat{q}_z z^2) (\int_{\sqrt{\hat{q}_z}}^{\infty} \mathcal{D}x)^{-1}.$$

As $\hat{q}_z \rightarrow 1$ it diverges, meaning $q_z \rightarrow +\infty$. Consequently, $\mathbf{q}_{\text{in}} = (q_x = B^{-1}, \hat{q}_x = +\infty, q_z = +\infty, \hat{q}_z = 1)$ is solution of the stationary equations for the BEC channel and any ρ , and thus $E_f = 0$. The same argument can be extended to other binary input channels (BSC, ZC, etc.); we confirm this numerically in Fig. 1. To show it analytically, the concrete expressions of the (right-hand side of the) q_z -stationary equation for other channels are found in table I of [3] (with the variable substitution $1 - \hat{q}_z \rightarrow E$). Instead, for the AWGNC with signal-to-noise ratio γ the q_z -stationary equation is $\gamma/(1 + \gamma(1 - \hat{q}_z))$ which does *not* diverge when $\hat{q}_z \rightarrow 1$. Thus $E_f > 0$; however $\lim_{B \rightarrow +\infty} E_f = 0$, see [9].

V. CAPACITY ACHIEVEMENT AS $B \rightarrow +\infty$

We now show that as the section size B diverges (after L is first taken to $+\infty$) the information-theoretic threshold R_{IT} tends to the Shannon capacity C for binary input channels, whenever a simple “spectral criterion” is verified:

Result 1. *Consider SS codes for any memoryless channel. Let the coding matrix \mathbf{A} be drawn from a rotational invariant ensemble, and whose empirical spectral measure converges to a well defined density with finite support as $L \rightarrow \infty$. The code is capacity achieving in the sense that $\lim_{B \rightarrow \infty} R_{\text{IT}} = C$ if and only if the asymptotic p.d.f. ρ_{supp} of the non-zero eigenvalues of $B^{-1}\mathbf{A}^\top \mathbf{A}$ verifies $\rho_{\text{supp}} \rightarrow \delta_1$ in law when $B \rightarrow \infty$, $\alpha \rightarrow 0$.*

According to this principle both the gaussian and row-orthogonal coding ensembles are capacity-achieving as $L \rightarrow +\infty$ followed by the large section size limit $B \rightarrow +\infty$. Note that for R to remain finite in this limit then necessarily $\alpha = \Theta(\ln B/B) \rightarrow 0$. The threshold R_{IT} extracted at finite section size B shown in Table I converges when B increases to their predicted asymptotics. The derivation of Result 1 is based on the analysis of the rescaled potential $\tilde{\Phi}_{\text{RS}} := \Phi_{\text{RS}}/\ln B$. One needs also to define rescaled parameters $r_x := Bq_x$ and $\hat{r}_x := \hat{q}_x/\ln B$ as in [9]. All the rescaled quantities have non-trivial limits as $B \rightarrow +\infty$. We now propose an heuristic (numerically verified) argument –which will be formalized in a longer version; see [1, 9] for related arguments– showing that as $B \rightarrow +\infty$ the potential $\tilde{\Phi}_{\text{RS}}$ possesses only two maxima,

one verifying $r_x = 1$ and another $r_x = 0$. The same holds in SS codes with gaussian coding matrices [6, 9, 10]. Indeed, the only term dependent on \hat{r}_x in $\tilde{\Phi}_{\text{RS}}$ is

$$\tilde{I}_0(r_x, \hat{r}_x) := I_0/\ln B \rightarrow \max(1, \hat{r}_x/2) - r_x \hat{r}_x/2 \quad (5)$$

as $B \rightarrow +\infty$; this was computed in [9]. Considering its \hat{r}_x -derivative to obtain the r_x -stationary equation, and given that $r_x \in [0, 1]$, it is clear that for r_x to possibly change its value (i.e., existence of two solutions) the “effective signal-to-noise” (SNR) \hat{r}_x must transition at $\hat{r}_x = 2$ (whatever is the solution of the $\tilde{\Phi}$ -stationary equations for the remaining parameters). So two scenarios are possible:

High error case: The effective SNR \hat{r}_x solution to the $\tilde{\Phi}_{\text{RS}}$ -stationary equations is low enough so that $\max(1, \frac{\hat{r}_x}{2}) = 1$. Then the r_x -stationary equation obtained by setting $\partial_{\hat{r}_x} \tilde{I}_0 = 0$ enforces $r_x = 0$ meaning no decoding at all (recall the link between overlap and MSE).

No error case: This time the solution \hat{r}_x is large enough so that $\max(1, \frac{\hat{r}_x}{2}) = \frac{\hat{r}_x}{2}$. Then $\partial_{\hat{r}_x} \tilde{I}_0 = 0$ yields the second solution $r_x = 1$, i.e., perfect decoding.

We argued that only two solutions exist and can now derive Result 1. From the definition of R_{IT} , we look for a rate such that $\tilde{\Phi}_{\text{RS}}(r_x = 0) = \tilde{\Phi}_{\text{RS}}(r_x = 1)$ (the other parameters being understood to be set at their respective solutions).

In the **no error case** $r_x = 1$ it is direct to see that $\mathcal{F}(x, y)$ is independent of ρ and thus $\mathcal{F} = \mathcal{F}_{\text{MP}}(x, y)$. As this is the only ρ -dependent part of the potential $\tilde{\Phi}_{\text{RS}}(r_x = 1) = \tilde{\Phi}_{\text{RS}}^{\text{MP}}(r_x = 1)$, the rescaled potential when considering the MP law ρ . As explained above, we also have $\tilde{I}_0(r_x = 1, \hat{r}_x) = 0$. We have seen in Sec. IV that perfect decoding implied the solution $\hat{q}_z = 1$ and $q_z = +\infty$ for any B (and thus in the limit). All-in-all it yields $\tilde{\Phi}_{\text{RS}}(r_x = 1) = \tilde{\Phi}_{\text{RS}}^{\text{MP}} = \frac{1}{R} \mathbb{E}_{z \sim \mathcal{N}(0,1)} \int dy P_{\text{out}}(y | z) \log_2 P_{\text{out}}(y | z)$ for this non error solution, and for any ρ .

Now the **high error case** $r_x = 0$. By [Lemma 1, [1]] the R -transform $\mathcal{R}(x)$ associated to a generic ρ [31] is upper bounded, when $B \rightarrow +\infty$, $\alpha \rightarrow 0$, by the one of the MP law. Then using the equivalent expression $\mathcal{F}(x, y) = \frac{1}{2} \inf_{\Lambda_y > 0} \{ \int_0^{-\frac{x}{\Lambda_y}} \mathcal{R}(t) dt + \alpha \Lambda_y y - \alpha \ln \Lambda_y - \alpha \ln y - \alpha \}$ we can show $\tilde{I}_{\text{int}} \geq \tilde{I}_{\text{int}}^{\text{MP}}$ where $\tilde{I}_{\text{int}} = \lim_B I_{\text{int}}/\ln B$. Because \tilde{I}_{int} is the only spectrum-dependent term of the potential we automatically deduce $\tilde{\Phi}_{\text{RS}} \geq \tilde{\Phi}_{\text{RS}}^{\text{MP}}$ when evaluated at the same solution (the high error one in that particular case). Equality holds if and only if $\rho \rightarrow \alpha \delta_1 + (1 - \alpha) \delta_0$ in law as $\alpha \rightarrow 0$. In the i.i.d. gaussian/MP ensemble $\mathcal{F}(x, y) = -\frac{\alpha}{2} xy$ which implies, when $r_x = 0$, $\tilde{I}_{\text{int}}^{\text{MP}} = 0$ independently of q_z . Because we also have $\tilde{I}_0 = 1$ for the high error solution, the lower bound on the replica potential reads $\tilde{\Phi}_{\text{RS}}^{\text{MP}}(r_x = 0) = 1 + \frac{1}{R} \int dy (\mathbb{E}_z P_{\text{out}}(y | z)) \log_2 \mathbb{E}_z P_{\text{out}}(y | z)$. From this “high error lower bound” $\tilde{\Phi}_{\text{RS}} = \epsilon_\rho + \tilde{\Phi}_{\text{RS}}^{\text{MP}}(r_x = 0)$ where $\epsilon_\rho \geq 0$, with equality if and only if $\rho \rightarrow \alpha \delta_1 + (1 - \alpha) \delta_0$ as $\alpha \rightarrow 0$.

R_{IT} is obtained by solving $\tilde{\Phi}_{\text{RS}}(r_x = 0) = \tilde{\Phi}_{\text{RS}}(r_x = 1)$. This yields $R_{\text{IT}} = \frac{1}{1 + \epsilon_\rho} [\mathbb{E}_z \int dy P_{\text{out}}(y | z) \ln_2 P_{\text{out}}(y | z) - \int dy (\mathbb{E}_z P_{\text{out}}(y | z)) \ln_2 (\mathbb{E}_z P_{\text{out}}(y | z))] = C/(1 + \epsilon_\rho)$. The coding scheme is thus capacity-achieving if and only if $\epsilon_\rho = 0$, i.e., $\rho_{\text{supp}} \rightarrow \delta_1$ in law when $\alpha \rightarrow 0$. This ends the argument.

ACKNOWLEDGMENTS

J.B and H.T.Q thank Nicolas Macris and Liang Shansuo for helpful discussions.

REFERENCES

- [1] TianQi Hou, YuHao Liu, Teng Fu, and Jean Barbier. Sparse superposition codes under vmp decoding with generic rotational invariant coding matrices, 2022.
- [2] Philip Schniter, Sundeep Rangan, and Alyson K Fletcher. Vector approximate message passing for the generalized linear model. In *2016 50th Asilomar Conference on Signals, Systems and Computers*, pages 1525–1529. IEEE, 2016.
- [3] Erdem Biyik, Jean Barbier, and Mohamad Dia. Generalized approximate message-passing decoder for universal sparse superposition codes. In *2017 IEEE International Symposium on Information Theory (ISIT)*, pages 1593–1597. IEEE, 2017.
- [4] Andrew R Barron and Antony Joseph. Toward fast reliable communication at rates near capacity with gaussian noise. In *2010 IEEE International Symposium on Information Theory*, pages 315–319. IEEE, 2010.
- [5] Andrew R Barron and Sanghee Cho. High-rate sparse superposition codes with iteratively optimal estimates. In *2012 IEEE International Symposium on Information Theory Proceedings*, pages 120–124. IEEE, 2012.
- [6] Jean Barbier, Mohamad Dia, and Nicolas Macris. Proof of threshold saturation for spatially coupled sparse superposition codes. In *2016 IEEE International Symposium on Information Theory (ISIT)*, pages 1173–1177. Ieee, 2016.
- [7] Cynthia Rush, Adam Greig, and Ramji Venkataramanan. Capacity-achieving sparse superposition codes via approximate message passing decoding. *IEEE Transactions on Information Theory*, 63(3):1476–1500, 2017.
- [8] Oliver Y Feng, Ramji Venkataramanan, Cynthia Rush, and Richard J Samworth. A unifying tutorial on approximate message passing. *arXiv preprint arXiv:2105.02180*, 2021.
- [9] Jean Barbier and Florent Krzakala. Approximate message-passing decoder and capacity achieving sparse superposition codes. *IEEE Transactions on Information Theory*, 63(8):4894–4927, 2017.
- [10] Jean Barbier, Mohamad Dia, and Nicolas Macris. Threshold saturation of spatially coupled sparse superposition codes for all memoryless channels. In *2016 IEEE Information Theory Workshop (ITW)*, pages 76–80. Ieee, 2016.
- [11] Antonia M Tulino, Giuseppe Caire, Sergio Verdú, and Shlomo Shamai. Support recovery with sparsely sampled free random matrices. *IEEE Transactions on Information Theory*, 59(7):4243–4271, 2013.
- [12] Junjie Ma, Xiaojun Yuan, and Li Ping. Turbo compressed sensing with partial dft sensing matrix. *IEEE Signal Processing Letters*, 22(2):158–161, 2014.
- [13] Jean Barbier, Nicolas Macris, Antoine Maillard, and Florent Krzakala. The mutual information in random linear estimation beyond iid matrices. In *2018 IEEE International Symposium on Information Theory (ISIT)*, pages 1390–1394. IEEE, 2018.
- [14] Junjie Ma, Ji Xu, and Arian Maleki. Analysis of sensing spectral for signal recovery under a generalized linear model. *Advances in Neural Information Processing Systems*, 34, 2021.
- [15] Marc Mezard and Andrea Montanari. *Information, physics, and computation*. Oxford University Press, 2009.
- [16] Mohsen Bayati and Andrea Montanari. The dynamics of message passing on dense graphs, with applications to compressed sensing. *IEEE Transactions on Information Theory*, 57(2):764–785, 2011.
- [17] Adel Javanmard and Andrea Montanari. State evolution for general approximate message passing algorithms, with applications to spatial coupling. *Information and Inference: A Journal of the IMA*, 2(2):115–144, 2013.
- [18] Parthe Pandit, Mojtaba Sahraee-Ardakan, Sundeep Rangan, Philip Schniter, and Alyson K Fletcher. Inference with deep generative priors in high dimensions. *IEEE Journal on Selected Areas in Information Theory*, 1(1):336–347, 2020.
- [19] Takashi Takahashi and Yoshiyuki Kabashima. Macroscopic analysis of vector approximate message passing in a model-mismatched setting. *IEEE Transactions on Information Theory*, 2022.
- [20] Jean Barbier, Nicolas Macris, Mohamad Dia, and Florent Krzakala. Mutual information and optimality of approximate message-passing in random linear estimation. *IEEE Transactions on Information Theory*, 66(7):4270–4303, 2020.
- [21] Galen Reeves and Henry D Pfister. The replica-symmetric prediction for compressed sensing with gaussian matrices is exact. In *2016 IEEE International Symposium on Information Theory (ISIT)*, pages 665–669. IEEE, 2016.
- [22] Jean Barbier, Florent Krzakala, Nicolas Macris, Léo Miolane, and Lenka Zdeborová. Optimal errors and phase transitions in high-dimensional generalized linear models. *Proceedings of the National Academy of Sciences*, 116(12):5451–5460, 2019.
- [23] Jean Barbier and Florent Krzakala. Replica analysis and approximate message passing decoder for superposition codes. In *2014 IEEE International Symposium on Information Theory*, pages 1494–1498. IEEE, 2014.
- [24] Marc Lelarge and Léo Miolane. Fundamental limits of symmetric low-rank matrix estimation. *Probability Theory and Related Fields*, 173(3):859–929, 2019.
- [25] Mohamad Dia, Nicolas Macris, Florent Krzakala, Thibault Lesieur, Lenka Zdeborová, et al. Mutual information for symmetric rank-one matrix estimation: A proof of the replica formula. *Advances in Neural Information Processing Systems*, 29, 2016.
- [26] Cedric Gerbelot, Alia Abbata, and Florent Krzakala. Asymptotic errors for teacher-student convex generalized linear models (or: How to prove kabashima’s replica formula). *arXiv preprint arXiv:2006.06581*, 2020.
- [27] Takashi Shinzato and Yoshiyuki Kabashima. Perceptron capacity revisited: classification ability for correlated patterns. *Journal of Physics A: Mathematical and Theoretical*, 41(32):324013, 2008.
- [28] Antoine Maillard, Bruno Loureiro, Florent Krzakala, and Lenka Zdeborová. Phase retrieval in high dimensions: Statistical and computational phase transitions. *Advances in Neural Information Processing Systems*, 33:11071–11082, 2020.
- [29] Antoine Maillard, Florent Krzakala, Yue M Lu, and Lenka Zdeborová. Construction of optimal spectral methods in phase retrieval. *arXiv preprint arXiv:2012.04524*, 2020.
- [30] Burak Çakmak and Manfred Opper. A dynamical mean-field theory for learning in restricted boltzmann machines. *Journal of Statistical Mechanics: Theory and Experiment*, 2020(10):103303, 2020.
- [31] Antonia M Tulino, Sergio Verdú, et al. Random matrix theory and wireless communications. *Foundations and Trends® in Communications and Information Theory*, 1(1):1–182, 2004.